

Supporting Information for the manuscript entitled:

Ordered crown-ether 2D framework based loose nanofiltration membranes for improved separation and stability

Jae Jun Kim^a, Huiran Seo^a, Jinseok Kim^a, Mun Hyeon Kim^a, Jinwook Park^a, Hyunkee Hong^a, Hee Joong Kim^{b,*}, and Jong-Chan Lee^{a,*}

^aDepartment of Chemical and Biological Engineering and Institute of Chemical Processes, Seoul National University, 1 Gwanak-ro, Seoul, 08826, Republic of Korea

^bDepartment of Polymer Science and Engineering & Program in Environmental and Polymer Engineering, Inha University, Incheon, 22212, Republic of Korea

List of contents

Figure S1. ^{13}C CP-MAS NMR and PXRD of C_2O structure -----	8
Figure S2. ^1H -NMR spectra of QDMAEMA -----	9
Figure S3. ^1H -NMR spectra of PQDMAEMA -----	10
Figure S4. Lattice fringe TEM images of C_2O , $\text{C}_2\text{O-Br}$ and $\text{C}_2\text{O-PQDM}$ -----	11
Figure S5. TGA curves of C_2O , $\text{C}_2\text{O-Br}$ and $\text{C}_2\text{O-PQDM}$ -----	12
Figure S6. XPS analysis of $\text{C}_2\text{O-Br}$ and $\text{C}_2\text{O-PQDM}$ -----	13
Figure S7. XPS analysis of $\text{LC}_2\text{O5}$ membrane -----	14
Figure S8. AFM images of LC_2O membranes -----	15
Figure S9. Cross-sectional SEM images of LC_2O membranes -----	16
Figure S10. Surface SEM images of LC_2O membranes -----	17
Figure S11. SEM-EDS images for LC_2O membranes -----	18
Figure S12. UV-Vis absorbance spectra of feed and permeate -----	19
Figure S13. Membrane performance upon filtration of Na_2SO_4 and MgSO_4 -----	20
Figure S14. Membrane performance of $\text{LC}_2\text{O5}$ using dyes/ NaCl solution -----	21
Figure S15. Membrane performance of $\text{LC}_2\text{O9}$ and L9 upon filtration of dye solution -----	22
Figure S16. Membrane performance of $\text{LC}_2\text{O5}$ with different model pollutants and concentration (CR , Na_2SO_4) -----	23
Table S1. Atomic compositions from XPS analysis of C_2O , $\text{C}_2\text{O-Br}$ and $\text{C}_2\text{O-PQDM}$ -----	24
Table S2. Elemental analysis of $\text{C}_2\text{O-PQDM}$ -----	25
Table S3. Zeta potential of $\text{C}_2\text{O-PQDM}$ solution -----	26

Table S4. Surface roughness values of membranes -----	27
Table S5. Properties of the dyes used in this study-----	28
Table S6. Calculation of EBT/NaCl selectivity for LC ₂ O membranes -----	29
Table S7. Comparison of the performance of LC ₂ O membrane with other literature -----	30

Experimental Section

Materials –The C₂O was synthesized by the self-condensation reaction of trichlorophloroglucinol as described in previous study.¹ The polyacrylonitrile (PAN) ultrafiltration membrane was obtained from Shandong Megavision Membrane Technology & Engineering Co., Ltd. Methyl blue (MB), eriochrome black T (EBT), methyl orange (MO), 2-(dimethylamino)ethyl methacrylate (DMAEMA), iodoethane, hydroquinone, 2-bromo-2-methylpropionyl bromide, copper(I) bromide, N,N,N',N'',N''-pentamethyldiethylenetriamine, Poly(sodium 4-styrenesulfonate) (PSS, average M_w = 70,000) were purchased from Merck (Sigma-Aldrich). 2,2'-Azobis(isobutyronitrile) (AIBN) was purchased from Merck (Sigma-Aldrich) and recrystallized in ethanol before use. Congo red (CR), metanil yellow (MY), triethylamine (TEA) were from Tokyo Chemical Industry (TCI). All other chemicals were used as received from commercial suppliers unless otherwise specified.

Synthesis of C₂O-Br –The C₂O (0.30 g) was dispersed in 30 mL of dimethylformamide (DMF) by sonication for 0.5 h and the solution was transferred to a one-neck round-bottom flask with a magnetic stirring bar. Triethylamine (2.43 g, 24 mmol) and 2-bromo-2-methylpropionyl bromide (4.05 g, 17.6 mmol) were added to the solution and stirred at 40 °C for 12 h. After the reaction, the crude solution was washed with methanol several times and dried in a vacuum oven at 60 °C for 24 h.

Preparation of the quaternized 2-(dimethylamino)ethyl methacrylate (QDM) –DMAEMA (15.0 g, 95 mmol), iodoethane (16.37 g, 105 mmol), hydroquinone (0.08 g, 0.73 mmol) and a magnetic stir bar were placed in a 250 mL round-bottom flask, followed by adding 50 mL of acetonitrile. Reaction was carried out at 45 °C for 18 h, and the crude solution was precipitated into diethyl ether several times. Subsequently, the product was obtained via filtration using a nylon filter (pore size, 0.2 μm), and dried in a vacuum oven at 30 °C for 24 h, yielding a white powder (Figure S1). ¹H NMR (400 MHz, DMSO-*d*₆, 25 °C) of QDM: δ [ppm] = 4.52 (COO-CH₂), 3.69 (CH₂-CH₂-O), 3.46 (CH₂-CH₂-N⁺(CH₃)₂), 1.91 (N⁺-CH₂-CH₃).

Synthesis of C₂O-PQDM –The C₂O-Br (0.08 g) was dispersed in 7.5 mL of dimethylformamide (DMF) by sonication for 0.5 h, and the solution was transferred to a 100 mL Schlenk flask equipped with a magnetic stirring bar. Subsequently, QDM (1.53 g, 4.9 mmol) was added into the solution. Copper(I) bromide (0.070 g, 0.48 mmol) was added to the flask, followed by three freeze-pump-thaw cycles. N,N,N',N'',N''-Pentamethyldiethylenetriamine (0.084 g, 0.48 mmol) was added to the mixture, followed by an additional freeze-pump-thaw cycle. The solution was heated at 70 °C for 48 h. After the reaction, the crude solution was washed with methanol several times and obtained through filtration with a nylon filter (pore size, 0.2 μm). The product was dried in a vacuum oven at 60 °C for 24 h, yielding a brown powder.

Synthesis of PQDM –QDM (1.53 g, 4.9 mmol), AIBN (0.08 g, 0.49 mmol), 5 mL of dimethylformamide (DMF) and a stirring bar were transferred to a 100 ml round-bottom flask, followed by five freeze-pump-thaw cycles. Reaction proceeded at 70 °C for 18 h. The crude solution was washed with acetone and diethyl ether several times and collected via filtration with a nylon filter (pore size, 0.2 μm). The product was dried in a vacuum oven at 60 °C for 24 h, yielding a white powder (Figure S2). ¹H NMR (400 MHz, DMSO-*d*₆, 25 °C) of PQDM: δ [ppm] = 4.41 (COO-CH₂), 3.90 (CH₂-CH₂-O), 3.61 (CH₂-CH₂-N⁺(CH₃)₂), 1.35 (N⁺-CH₂-CH₃).

Fabrication of loose nanofiltration membrane –50 mg of C₂O-PQDM and/or PSS were dispersed in 100 ml DI water and stirred for 1 h to form a uniformly dispersed solution. Before the assembly process, the polyacrylonitrile (PAN) ultrafiltration membrane was hydrolyzed by immersion in a 2 M NaOH aqueous solution at 45 °C for 1 h, followed by rinsing with DI water. Subsequently, the hydrolyzed PAN membrane was immersed in the C₂O-PQDM solution at 40 °C for 15 min, and then rinsed with DI water. This was followed by immersion in the PSS solution at 40 °C for 15 min, and another rinse with DI water, forming a single layer of C₂O-PQDM/PSS. These immersing and rinsing steps were repeated to obtain the desired number of C₂O-PQDM/PSS layers on a PAN membrane. LC₂O# demonstrates C₂O-PQDM/PSS LbL membrane with # layers; for example, LC₂O5 membrane consists of five pairs of C₂O-PQDM/PSS layers. The LbL membrane prepared by only polyelectrolytes – PQDM and PSS – without C₂O was designated as L#.

Membrane filtration test –Membrane filtration tests were carried out using dead-end filtration cells (CF042, Sterlitech Corp., Kent, WA) with an effective filtration area of $1.3 \times 1.3 \times \pi \text{ cm}^2$. The experiment was operated under a pressure of 6 bar, and membranes were pre-pressurized for 0.5 h before test. The water and solution permeance was estimated by Eq. (1):

$$J (\text{L m}^{-2} \text{ h}^{-1} \text{ bar}^{-1}) = \Delta V / (A \times \Delta t \times P) \quad (1)$$

where ΔV is the volume of permeate (L), A is the effective area of membrane (m^2), Δt is the time taken to collect the permeate (h), and P is the operating pressure (bar).

The rejection (R) of salt or dye was estimated using 1000 ppm salt and/or 100 ppm dye feed solution and calculated by Eq. (2):

$$R (\%) = (1 - C_p / C_f) \times 100 \quad (2)$$

where C_f and C_p are the salt or dye concentration of the feed and permeate, respectively. The salt concentration was determined by a conductivity meter (HI 5321, Hanna instruments, USA). The dye concentrations were measured using a UV-Visible Spectrometer (U5100, Hitachi, Japan) at the maximal absorption wavelength of each dyes.

The separation factor S of the salt/dye mixture was calculated using Eq. (3).

$$S = (100 - R_{\text{salt}}) / (100 - R_{\text{dye}}) \quad (3)$$

where $R_{\text{dye}}(\%)$ and $R_{\text{salt}}(\%)$ are the rejection of dye and salt, respectively.

The chemical stability of the membrane was investigated using MB solutions under various pH conditions (pH 1, 3, 7, 11, 13). The measurement methods were identical to those used in the previous dye separation experiment.

Characterizations –The chemical structure was confirmed by $^1\text{H-NMR}$ and $^{13}\text{C CP-MAS}$ spectroscopy (Advance 400 FT-NMR, Bruker, USA) using $\text{DMSO-}d_6$ as an NMR solvent. Fourier-transform infrared spectroscopy (FT-IR, Nicolet 6700, Thermo Scientific, USA) was conducted to verify the chemical structure of materials and membranes. Thermogravimetric analysis (TGA,

Q50, TA Instrument, USA) was performed in the temperature range of 100–700 °C with a heating rate of 5 °C min⁻¹ under N₂ atmosphere to measure the thermal stability of materials. X-ray diffractions (XRD, D8 advance, Bruker, Germany) data was obtained to identify the crystallographic structures of the materials. X-ray photoelectron spectroscopy (XPS, AXIS-His, KRATOS, UK) with Al K α (1486.6 eV) radiation source was used to characterize the surface compositions of the materials and membranes. Field-emission scanning electron microscopy and energy dispersive X-ray spectroscopy (FE-SEM, SUPRA 55VP, Carl Zeiss, Germany) was carried out to examine the membrane surfaces. Transmission electron microscopy (TEM, JEM-F200, JEOL, Japan) was conducted with an accelerating voltage of 200 kV. Electrophoretic light scattering spectrophotometer (ELS Z-neo, Otsuka Electronics, Japan) was performed to measure the zeta potential of polycation solution. Zeta potential Analyzer (ELSZ-2000, Otsuka Electronics, Japan) was used to measure the surface zeta potential of membranes (at pH 6.4). Elemental Analyzer (EA, Flash2000, Thermo Scientific, USA) was carried out to determine the chemical composition of materials. The membranes' surface hydrophilicity was investigated via contact angle measurement in sessile drop mode. (DSA 25, KRUSS, Germany).

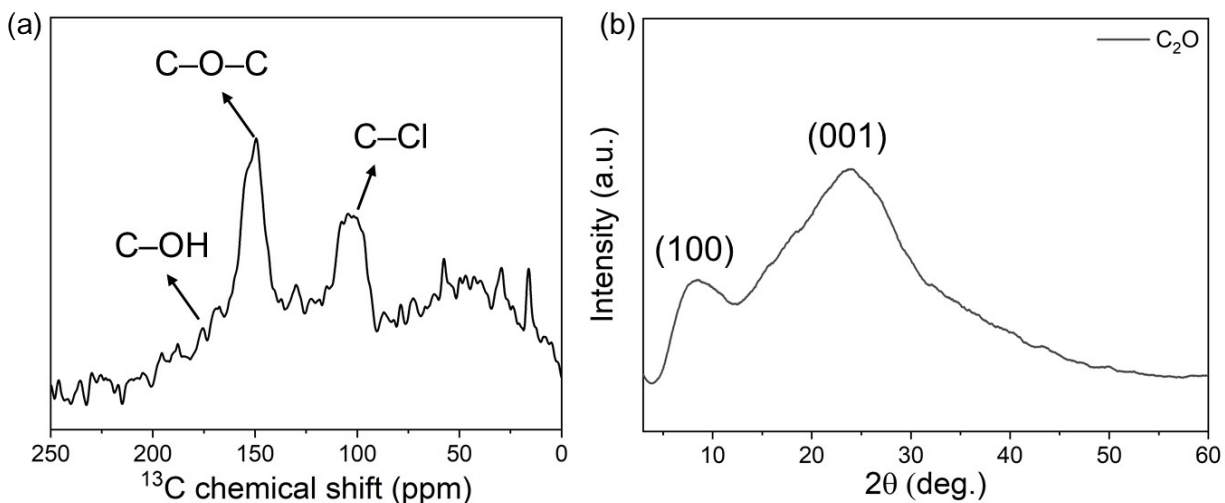


Figure S1. (a) ^{13}C CP-MAS NMR and (b) PXRD of C_2O structure.

The Solid-state ^{13}C cross-polarization magic-angle spinning (CP-MAS) NMR confirmed the chemical structure of C_2O , showing peaks for C-OH, C-O-C, and C-Cl at 175, 150, and 104 ppm, respectively. Additionally, powder X-ray diffraction (PXRD) analysis revealed two distinct peaks at 10° and 26° , corresponding to an in-plane reflection (100) of 0.88 nm and an interlayer distance (001) of 0.34 nm, confirming the crystalline structure of C_2O .

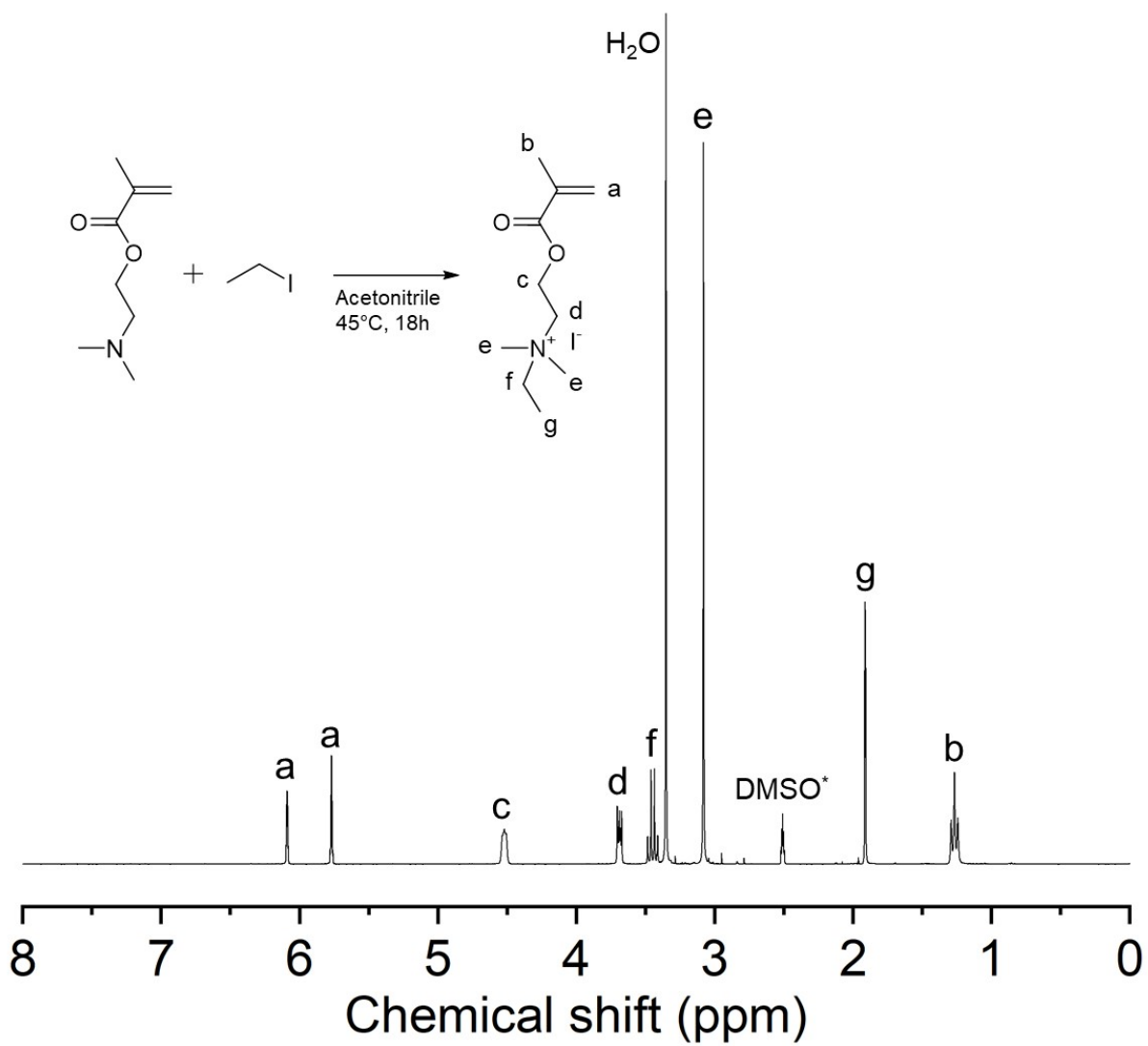


Figure S2. $^1\text{H-NMR}$ spectra of QDMAEMA.

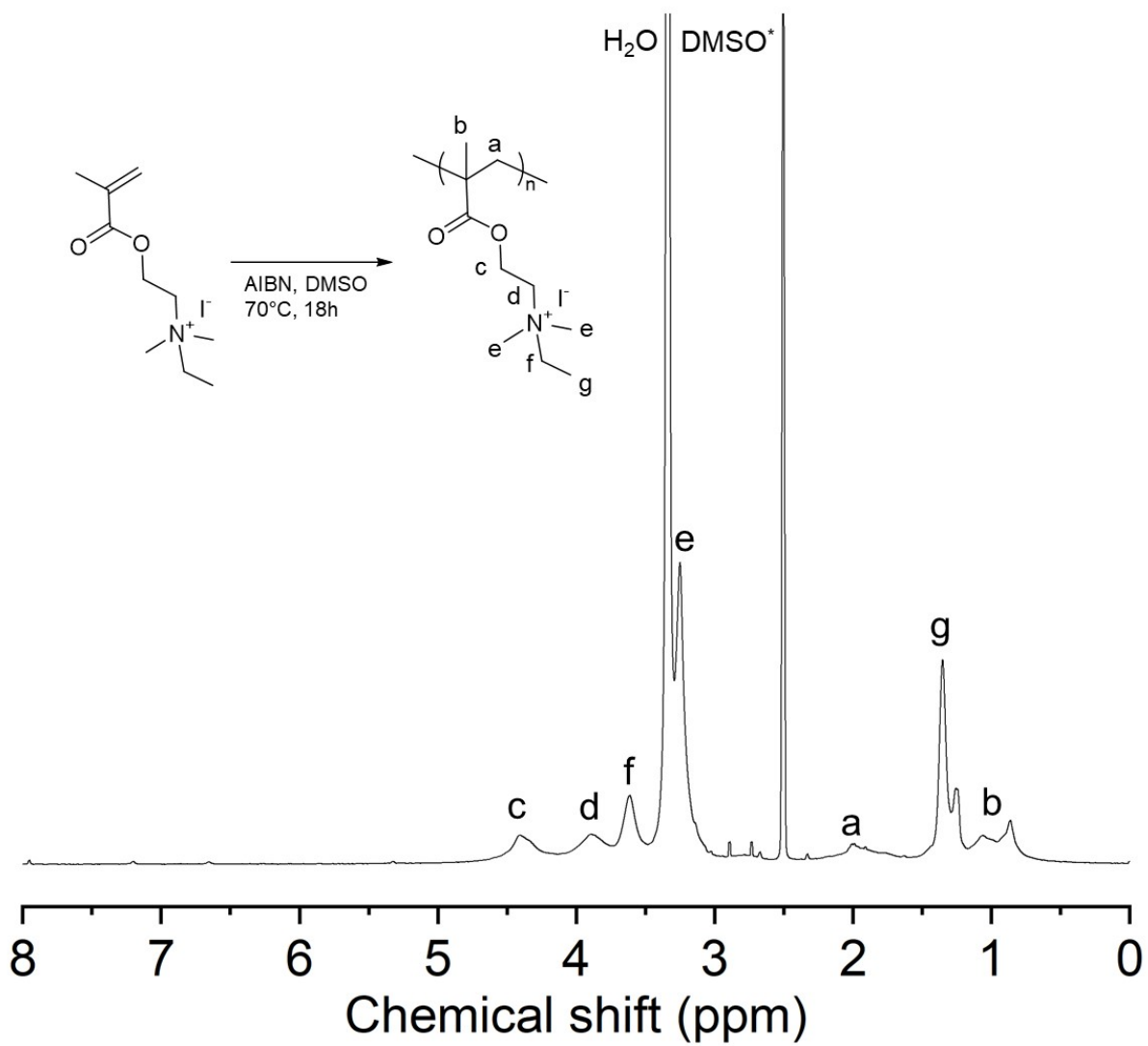


Figure S3. ¹H-NMR spectra of PQDM.

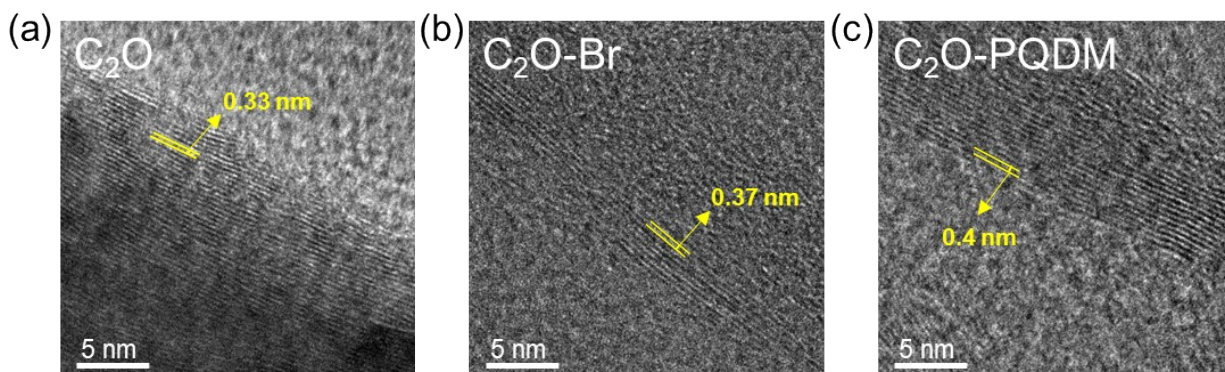


Figure S4. Lattice fringe TEM images: (a) C_2O , (b) C_2O-Br , and (c) $C_2O-PQDM$.

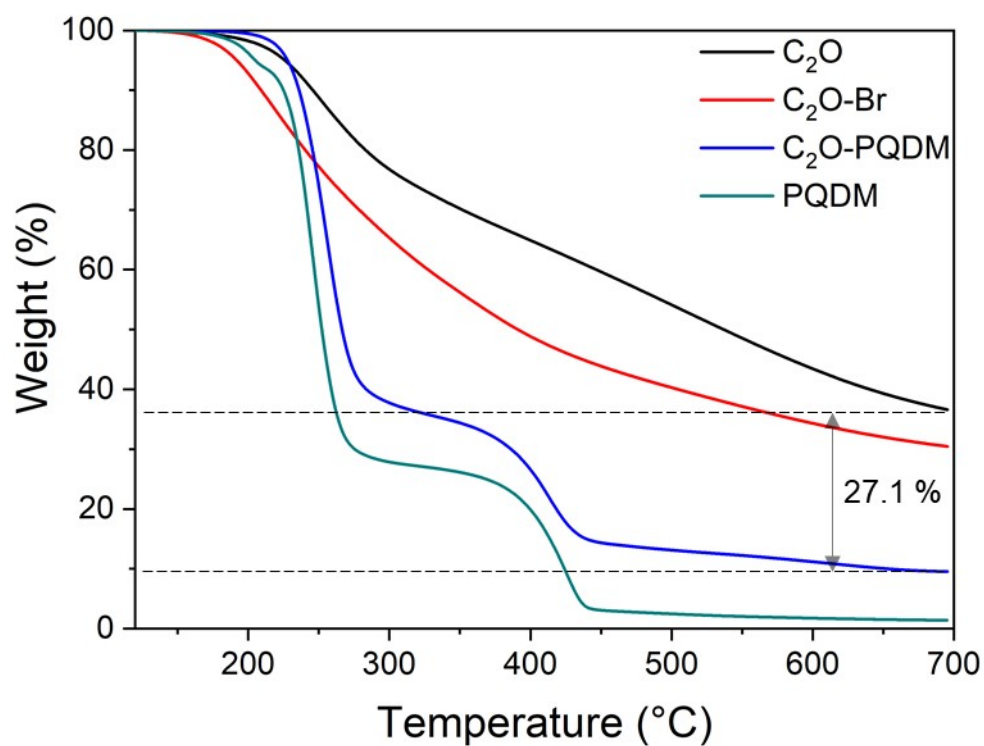


Figure S5. TGA curves of C₂O, C₂O-Br, and C₂O-PQDM.

The weight fractions of functional groups for C₂O-Br and C₂O-PQDM were analyzed by TGA. Slightly lower char yield of C₂O-Br compared to that of C₂O is due to the volatile Br groups. TGA data indicate that weight fraction of grafted polymer (i.e., PQDM) in C₂O-PQDM is about 78%, consistent with XPS data shown in Table S1.

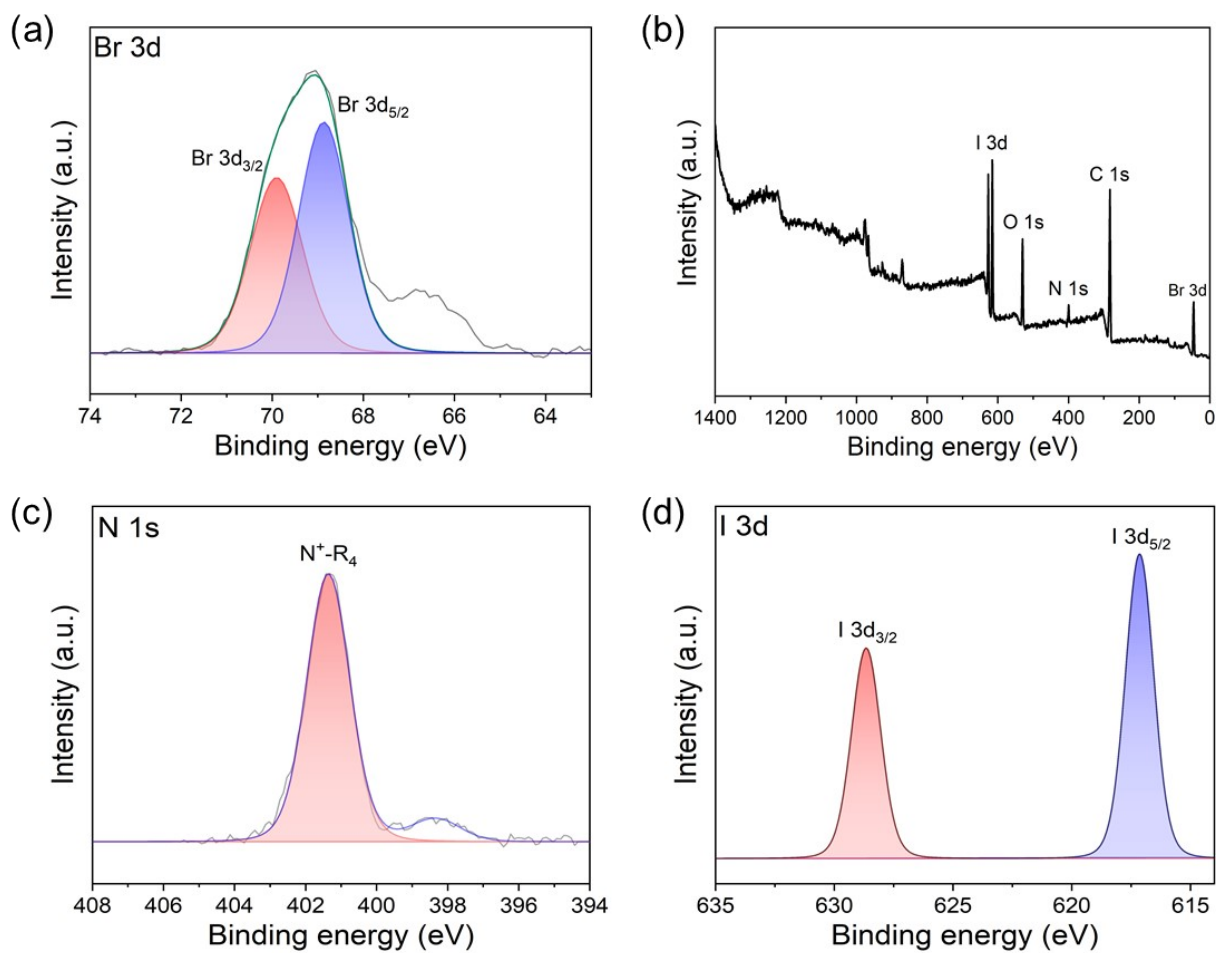


Figure S6. XPS spectra of (a) Br 3d of C₂O-Br, and (b) wide scan, (c) N 1s, (d) I 3d of C₂O-PQDM.

The chemical compositions of C₂O, C₂O-Br, and C₂O-PQDM were confirmed by XPS analysis. In the XPS spectra, the characteristic Br 3d peak was clearly detected in C₂O-Br, while in C₂O-PQDM, peaks corresponding to the C-N⁺ bond and the I 3d were observed.

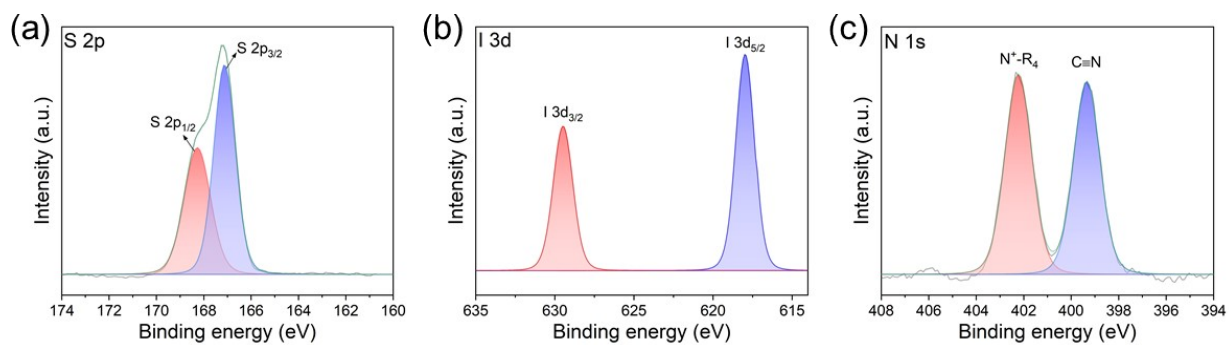


Figure S7. XPS spectra of (a) S 2p, (b) I 3d, and (c) N 1s of LC₂O₅ membrane.

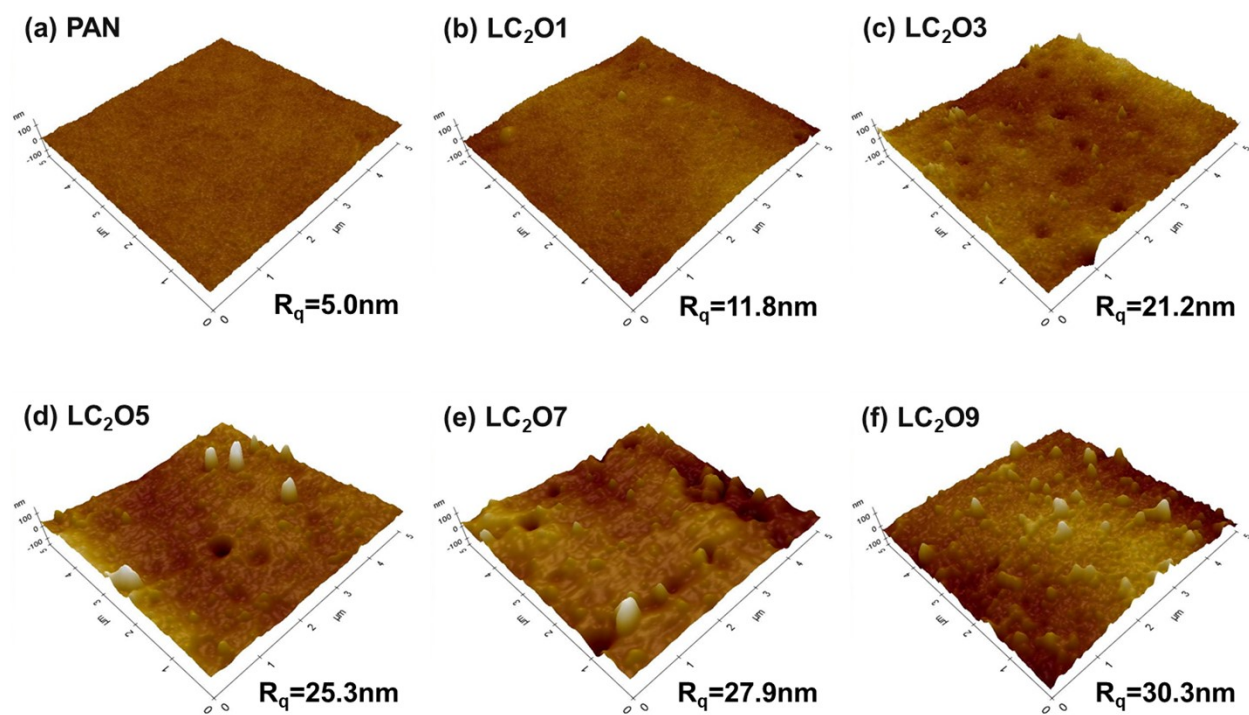


Figure S8. AFM images of (a) PAN, (b) LC₂O1, (c) LC₂O3, (d) LC₂O5, (e) LC₂O7, and (f) LC₂O9 membranes.

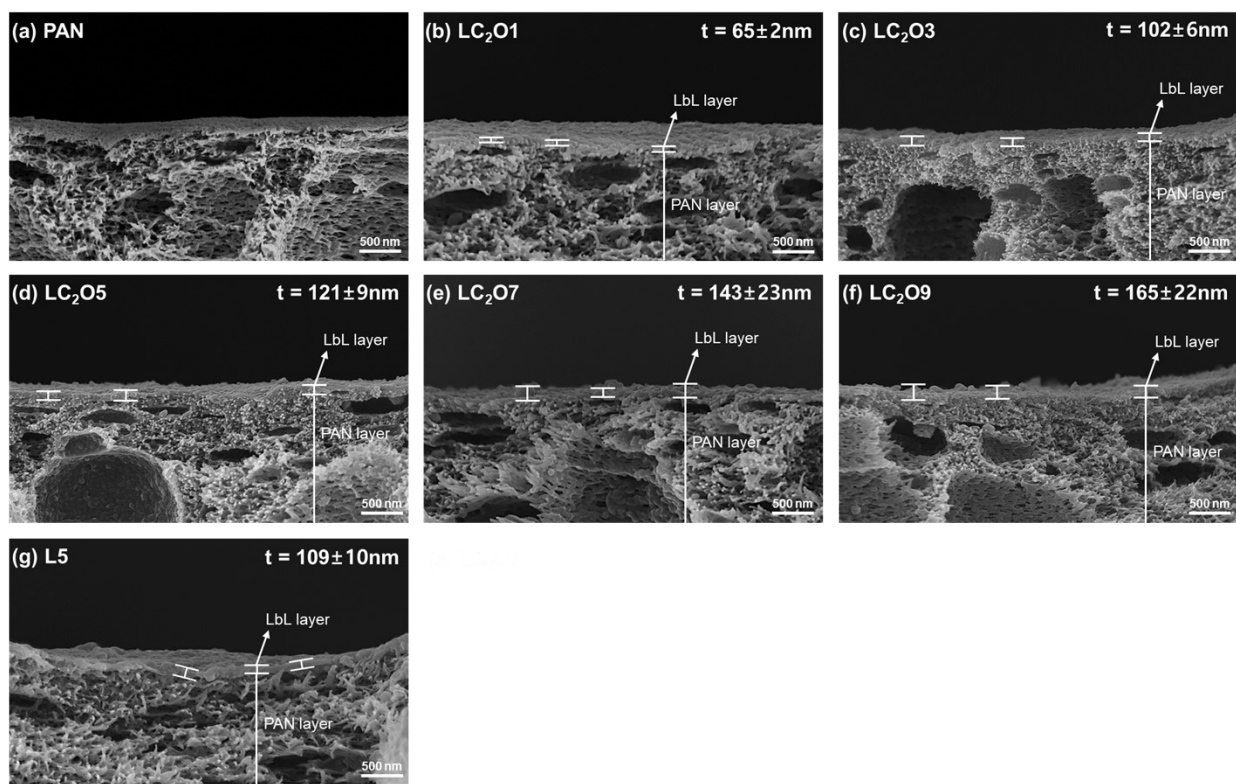


Figure S9. Cross-sectional SEM images of (a) PAN, (b) LC₂O1, (c) LC₂O3, (d) LC₂O5, (e) LC₂O7, (f) LC₂O9, and (g) L5 membranes.

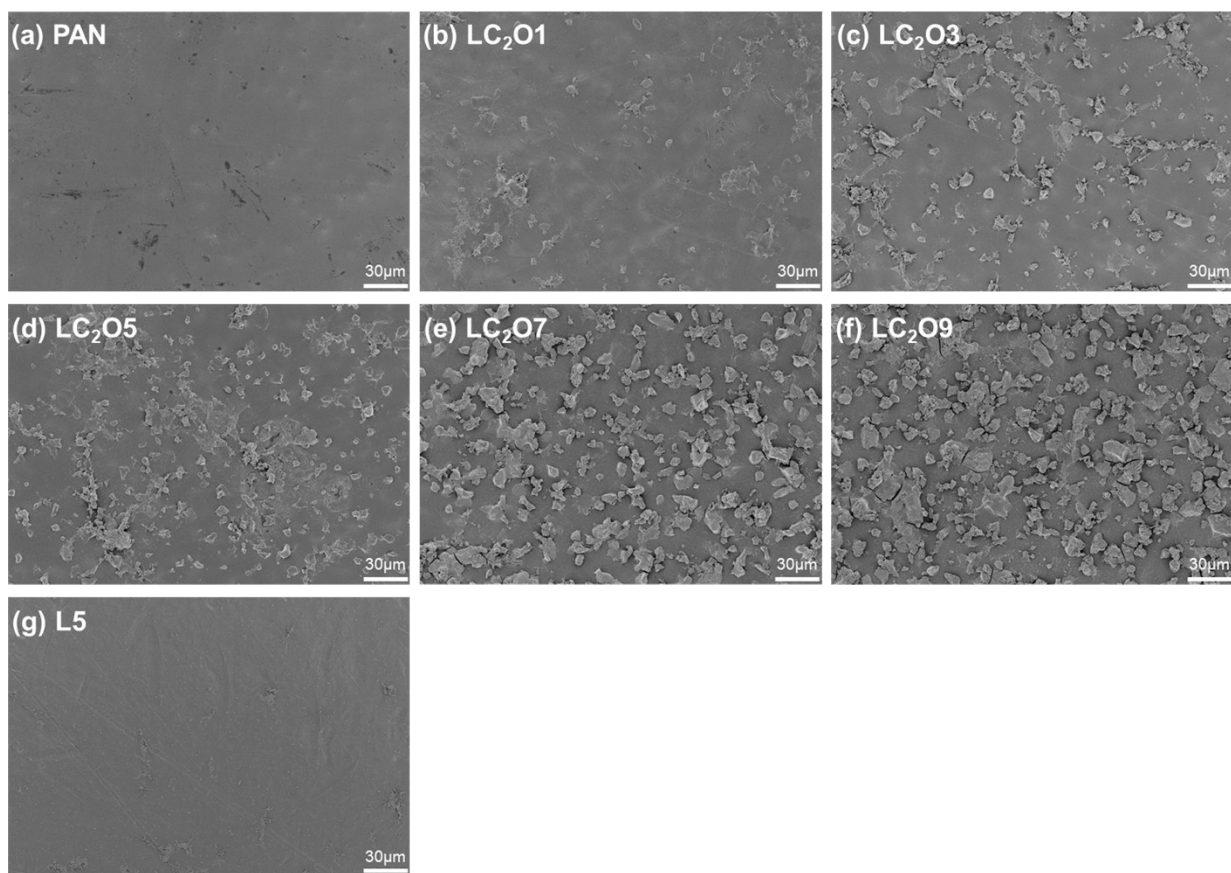


Figure S10. Surface SEM images of (a) PAN, (b) LC₂O1, (c) LC₂O3, (d) LC₂O5, (e) LC₂O7, (f) LC₂O9, and (g) L5 membranes.

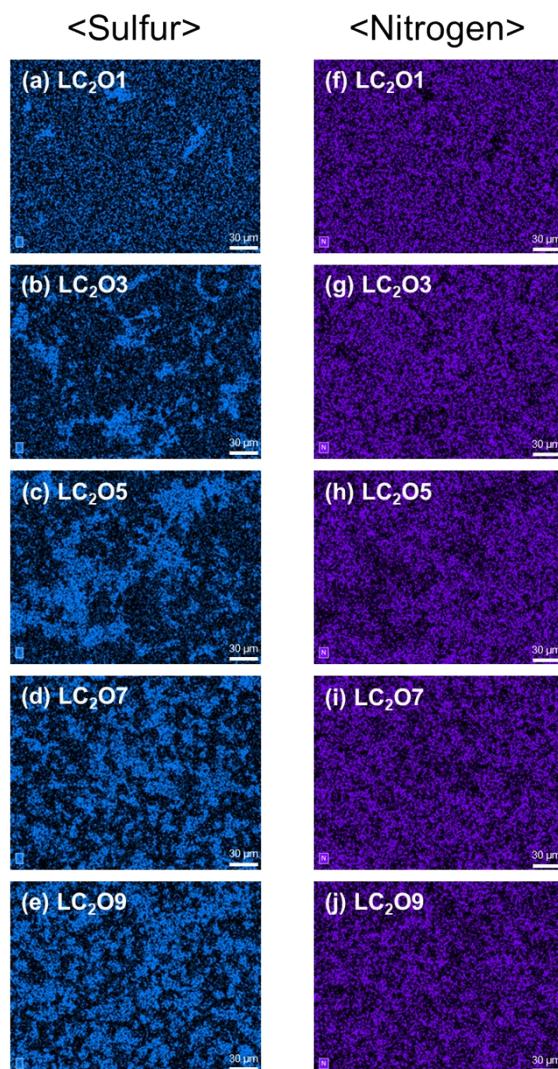


Figure S11. SEM-EDS images for LC₂O# membranes: (a-e) sulfur and (f-j) nitrogen component.

SEM energy dispersive X-ray spectroscopy (EDS) was performed to analyze the distribution of sulfur and nitrogen in the LC₂O# membranes. The sulfur content increased with the number of layers, confirming the increased deposition of PSS. PSS interacts with C₂O in C₂O-PQDM through π - π interactions and Van der Waals forces, or with PQDM through electrostatic interactions, ensuring a uniform distribution despite some degree of aggregation.

As for nitrogen, no significant differences were observed across the LC₂O# membranes, as the PAN support layer also contains nitrile group, which may mask variations in PQDM deposition. These results support that both PSS and C₂O-PQDM are functioning as intended in the membrane structure, and the stacking does not affect the nanofiltration performance.

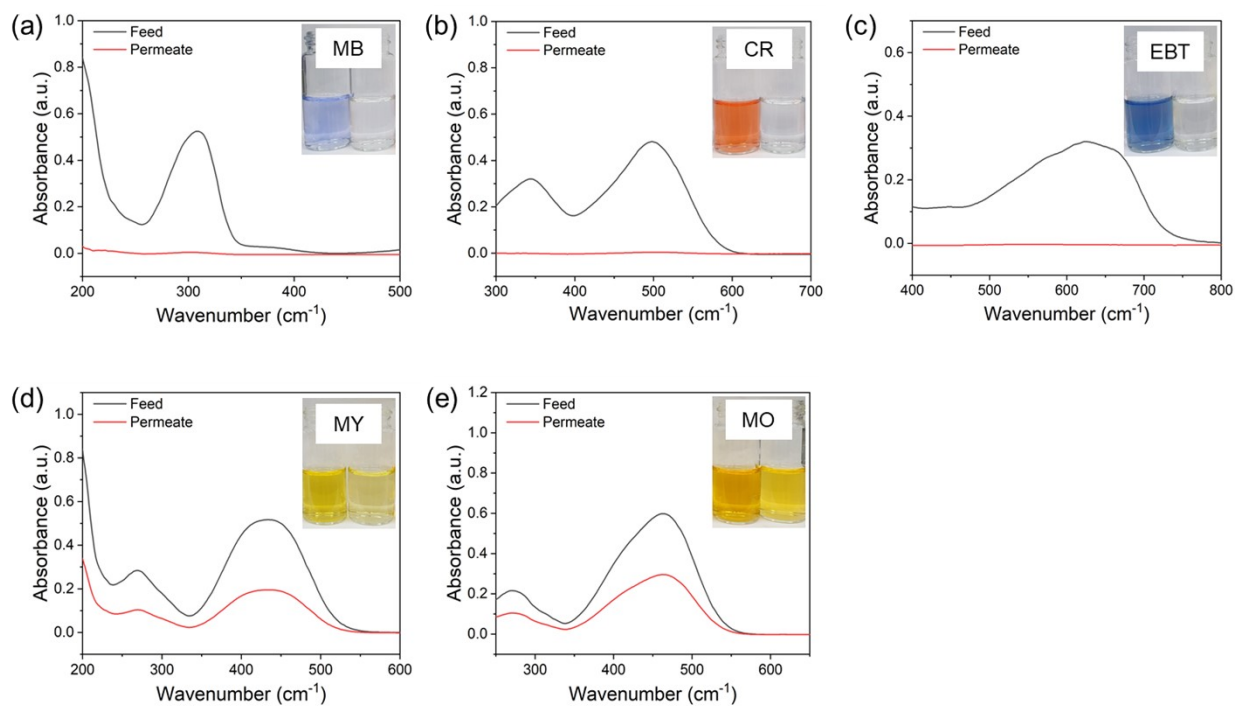


Figure S12. UV-Vis absorbance spectra of feed and permeate: Filtration of dyes through the $\text{LC}_2\text{O5}$ membrane.

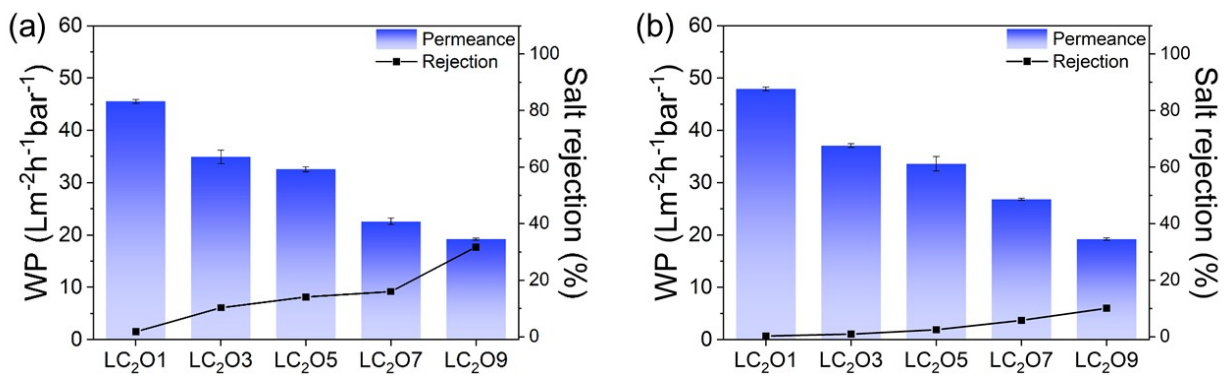


Figure S13. Membrane performance upon filtration of (a) Na₂SO₄ and (b) MgSO₄.

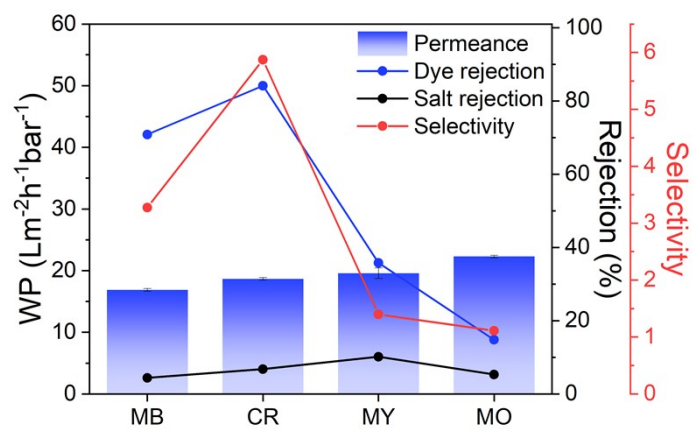


Figure S14. Membrane performance of LC₂O5 using dyes/NaCl solution.

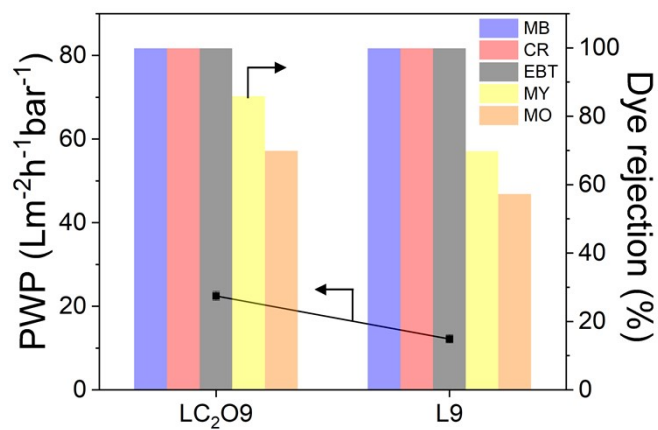


Figure S15. Membrane performance of LC₂O9 and L9 upon filtration of dye solution.

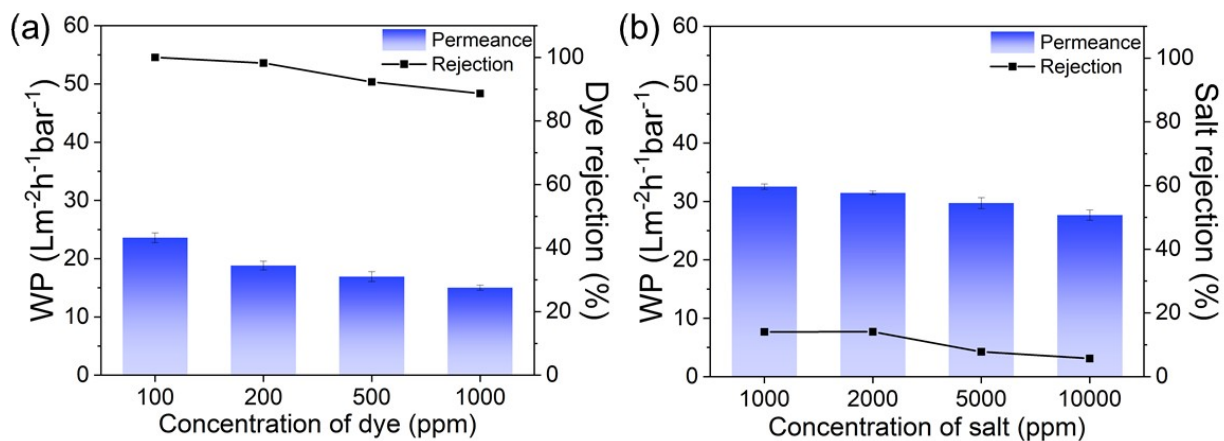


Figure S16. Membrane performance of LC₂O₅ with different model pollutants and concentration: (a) CR and (b) Na₂SO₄.

Table S1. Atomic compositions from XPS analysis of C₂O, C₂O-Br, and C₂O-PQDM.

materials	Atomic compositions (At.%)					
	C	N	O	Cl	Br	I
C ₂ O	72.77	-	24.27	2.96	-	-
C ₂ O-Br	77.51	-	21.45	0.58	0.46	-
C ₂ O-PQDM	79.04	3.81	13.4	-	0.66	3.1

Table S2. Elemental analysis result of C₂O-PQDM.

Sample	Carbon (wt%)	Hydrogen (wt%)	Nitrogen (wt%)
C ₂ O-PQDM	36.4323	6.3035	4.0458

Table S3. Zeta potential of C₂O-PQDM solution.

Solution	Concentration (mg/ml)	Zeta potential (mV)
C ₂ O-PQDM	0.5	34.57±0.14

Table S4. Surface roughness values of PAN and LC₂O membranes.

	PAN	LC ₂ O1	LC ₂ O3	LC ₂ O5	LC ₂ O7	LC ₂ O9
R_q (nm)	5.0	11.8	21.2	25.3	27.9	30.3
R_a (nm)	3.9	9.1	16.5	17.1	20.9	23.9

Table S5. Properties of the dyes used in this study.

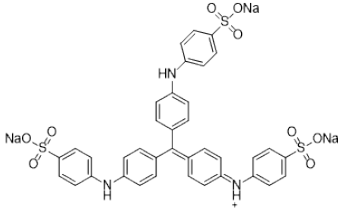
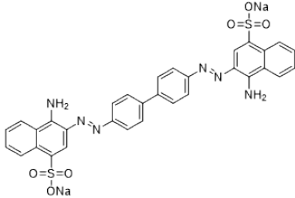
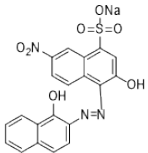
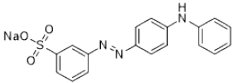
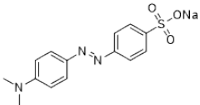
Dye name	Molecular structure	Molecular weight (Da)	Molecular size (nm)	λ_{\max} (nm)
Methyl blue (MB)		799	2.21 × 0.93	310
Congo red (CR)		696	2.41 × 0.75	498
Eriochrome Black T (EBT)		461	1.53 × 0.81	625
Metanil yellow (MY)		375	-	435
Methyl orange (MO)		327	1.51 × 0.43	465

Table S6. Calculation of EBT/NaCl selectivity for LC₂O# membranes.

	LC ₂ O1	LC ₂ O3	LC ₂ O5	LC ₂ O7	LC ₂ O9
NaCl rejection (%)	7.5	9.6	11.6	12.0	12.8
EBT rejection (%)	90.7	93.5	99.7	99.7	99.7
Selectivity	10.0	13.8	294.7	293.3	290.7

Table S7. Comparison of the performance of LC₂O membrane with other literature.

Membrane	PWP (L m ⁻² h ⁻¹ bar ⁻¹)	Dye rejection (%)	Operating pressure (bar)	Ref.
(TA/JA) ₂ /PAN	37	CR: 99.5% MB: 98%	2	2
(PEI/SCF) _{4.5} /PAN	24.3	RdB: 93.7% EbT: 90.8%	4	3
(PEI/GO) ₃ /PK	3.98	MLB: 85.1% RB: 99.9%	6	4
(M-CP) ₅ /PVDF	25	CR: >99.5%	2.75	5
(PDDA/GO) ₄ /PAN	6.2	MB: 99.2%	5	6
(TA/Fe ³⁺) ₅ /PAN	40.9	CR: 98.9%	2	7
(TA/PEPA) _{1.5} /PES	46.52	CR: >97%	2.5	8
(PEI-PO ₃ Na/PEI)/PES	24.2	VB: 99.5%	2	9
LC ₂ O5/PAN	39.1	CR: >99%	5	This study

References

1. J. Kim, S. Kim, J. Park, S. Kang, D. J. Seo, N. Park, S. Lee, J. J. Kim, W. B. Lee, J. Park and J.-C. Lee, *J. Am. Chem. Soc.*, 2024, **146**, 4532-4541.
2. D. Guo, Y. Xiao, T. Li, Q. Zhou, L. Shen, R. Li, Y. Xu and H. Lin, *J. Colloid Interface Sci.*, 2020, **560**, 273-283.
3. H. Guo, M. Chen, Q. Liu, Z. Wang, S. Cui and G. Zhang, *Desalination*, 2015, **365**, 108-116.
4. C. Wang, M. J. Park, R. R. Gonzales, H. Matsuyama, E. Drioli and H. K. Shon, *Desalination*, 2023, **549**, 116357.
5. U. S. Joshi, Anuradha and S. K. Jewrajka, *J. Membr. Sci.*, 2023, **669**, 121286.
6. L. Wang, N. Wang, J. Li, J. Li, W. Bian and S. Ji, *Sep. Purif. Technol.*, 2016, **160**, 123-131.
7. Y. Xiao, D. Guo, T. Li, Q. Zhou, L. Shen, R. Li, Y. Xu and H. Lin, *Appl. Surf. Sci.*, 2020, **515**, 146063.
8. X. Luo, S. Feng, Z. Zhang, L. Liu, L. Wu and C. Zhang, *J. Mater. Sci.*, 2022, **57**, 9002-9017.
9. S. Xiong, C. Han, A. Phommachanh, W. Li, S. Xu and Y. Wang, *Sep. Purif. Technol.*, 2021, **274**, 119105.